Mededelingen van de Koninklijke
Academie voor Wetenschappen, Letteren
en Schone Kunsten van België

Overdruk uit

Academiae Analecta

AWLSK

Klasse der Wetenschappen, Jaargang 53, 1991, Nr. 1

Paleis der Academiën, Brussel

APPROXIMATE AND NUMERICAL METHODS IN ACOUSTO-OPTICS
PART II. OBLIQUE INCIDENCE OF THE LIGHT BRAGG REFLECTION *

BY

Robert A. MERTENS **, Willy HEREMAN †
and Jean-Pierre OTTOY ‡

* An extended version of a lecture given by R.A. Mertens at the Class of Sciences on October 11, 1989. In addition to a survey of known methods, the paper comprises the latest results of original and unpublished research by the present authors.

** Instituut voor Theoretische Mechanika, Rijksuniversiteit Gent, Krijgslaan 281, B-9000 Gent (Belgium), member of the Academy.

† Department of Mathematical and Computer Sciences, Colorado School of Mines, Golden, CO 80401, USA.

‡ Seminarie voor Toegepaste Wiskunde en Biometrie, Rijksuniversiteit Gent, Coupure Links 653, B-9000 Gent (Belgium)

Dankwoord — Acknowledgements

R.A.M. wenst zijn dank te betuigen aan het Nationaal Fonds voor Wetenschappelijk Onderzoek van België voor een krediet aan navorsers.

He also thanks the Mathematics Department and the Center for Mathematical Sciences of the University of Wisconsin at Madison (USA) for their hospitality. He further wishes to thank Professor A. Korpel for a stay at the Department of Electrical and Computer Engineering of the University of Iowa at Iowa City (USA) and for fruitful discussions. W.H. gratefully acknowledges support from the US Air Force Office of Scientific Research under Grant No 85-NM-0263.

Een bijzonder woord van dank gaat naar de heer H. Vermis voor het zorgvuldig LaTeXen van het manuskript en naar de heer V. Ros voor het tekenen van de talrijke uitstekende figuren en grafieken en voor hun fotografische reproduktie.

We wish to express our gratitude to Prof. O. Leroy and Dr. E. Blomme for bringing a paper by W. G. Mayer to our attention and also for giving us access to their latest results prior to publication.

Introduction

In Part I [64][1] we briefly reviewed the principles of acousto-optic diffraction and we discussed some approximate and numerical methods to treat this problem in the case of normal incidence of the light. Particularly the NOA method and its reduction to an eigenvalue problem were studied in detail. Our theoretical formulae for the intensities of zeroth and first order proved to fit the experimental data of Klein and Hiedemann [22]. The accuracy of the computer calculations based on these formulae for intensities of higher order (up to the 9th) was also confirmed by experiments by Defèbvre [59,60] for acoustical frequencies of 1, 3 and 5 MHz, for a wide range of values of the Klein-Cook parameter Q. This near perfect agreement between theory and experiment encouraged us to extend the NOA method and its associated eigenvalue problem to the case of oblique incidence of the light.

We recall the basic Raman-Nath (RN) equations for oblique incidence of the light, i.e. Eq. (20) in Part I :

$$2\frac{d\phi_n}{d\zeta} - (\phi_{n-1} - \phi_{n+1}) = in\,(n\rho - 2a\sin\varphi)\,\phi_n,\ n = 0,\pm1\pm2,..., \qquad (71)$$

[1] Reference numbers [1] through [54] refer to the bibliography in Part I. Sections, formulae, figures and new references will be successively numbered.

together with the boundary conditions (21),

$$\phi_n(0) = \delta_{n0} \ , \ n = 0, \pm 1, \pm 2, \ldots. \tag{72}$$

In practice $\varphi \ll 1$, thus $\cos \varphi \approx 1$, which in turn justifies to set $\zeta' \approx \zeta$, $\upsilon' \approx \upsilon$ and $Q' \approx Q$. Introducing the parameter

$$\beta = -\frac{2a}{\rho} \sin \varphi, \tag{73}$$

the system (71) can be compactly written as

$$2\frac{d\phi_n}{d\zeta} - (\phi_{n-1} - \phi_{n+1}) = i\rho n\,(n + \beta)\,\phi_n, \ n = 0, \pm 1, \pm 2, \ldots. \tag{74}$$

The choice $\beta = -p$, with p a nonzero integer, gives

$$\sin \varphi = p\frac{\rho}{2a} = p\frac{\lambda}{2\lambda^*} = \sin \varphi_{BR}^{(p)}, \ p = \pm 1, \pm 2, \ldots, \tag{75}$$

where we took into account the expressions for the parameters ρ and a, defined in (23) and (24).

Naturally, $\varphi_{BR}^{(p)}$ is called the Bragg angle of order p (see (25)). An interpretation of this angle for $p = 1$ was given in Part I as well.

For the Bragg angle of order p, the intensity of the pth order line in the diffraction spectrum, as a function of φ reaches a maximum. This property was shown by Brillouin [57] for $p = 1$ using a perturbation theory. Phariseau [66] also showed that I_1 reaches its maximum for perfect Bragg incidence ($p = 1$). He based his argument on the RN system (71) subject to the constraint $\rho \gg 1$. The general property, corresponding to *any* integer value of p, was proved by Plancke-Schuyten and Mertens in the framework of their GFM [68]. An interesting intuitive explanation was provided by Brillouin [57] and is sketched in Fig. 21. An acoustic wave produces in the medium a series of parallel planes, M_1, M_2, ..., at distance λ^*, at which the density of the medium is maximal, and planes m_1, m_2, ..., where the density is minimal. Parallel light waves I_1C_1, I_2C_2 , ... entering the planes M_1, M_2, ..., where the refraction index is clearly different from the mean refraction index of the surrounding medium, will emerge as the waves C_1R_1, C_2R_2 , ... Snell's law assures that the angle of incidence φ is equal to the angle of reflection. The light reflected from the successive planes will only have a notable intensity if the different reflected waves are in phase. This requires that the optical path difference of the rays R_1 and R_2 should be given by $AC_2B = 2\lambda^* \sin \varphi = p\lambda$ ($p = \pm 1, \pm 2, \ldots$) so that $\sin \varphi_{BR}^{(p)} = p\frac{\lambda}{2\lambda^*}$, where $\varphi_{BR}^{(p)}$ is the Bragg angle of order p defined in (75). This argument is analogous to the one often used in textbooks on crystallography for defining the Bragg angle for the diffraction of X-rays by a crystal lattice. In the latter case λ is the wavelength of the

X-rays and λ^* should be replaced by d, the distance between two successive planes of the crystal. This justifies the name *Bragg reflection* which incidentally plays an important role in acousto-optics with oblique incidence of the light which will become clear later on.

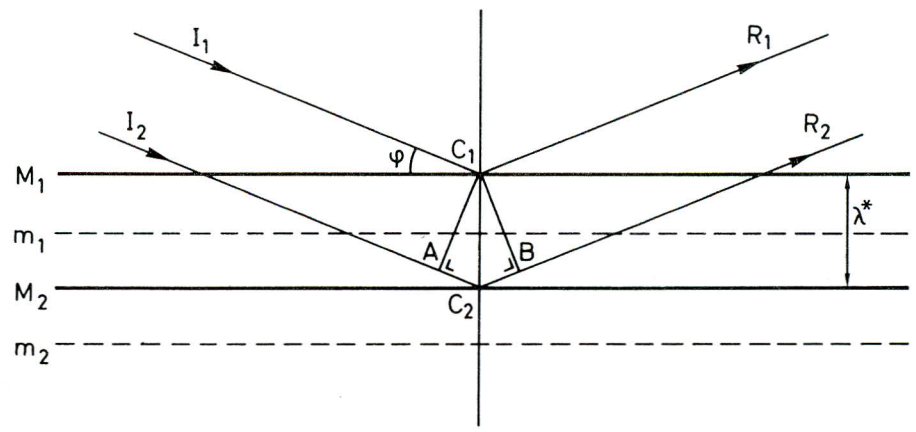

Fig. 21. Bragg reflection according to Brillouin's intuitive explanation.

The system (71) with boundary conditions (72) has been solved exactly by the GFM [67,68], leading to an infinite series for the amplitudes ϕ_n, containing the expansion coefficients of the Mathieu functions of fractional order, $ce_{n,\beta_1}(x,q)$, $se_{n,\beta_1}(x,q)$, $ce_{n,1-\beta_1}(x,q)$, $se_{n,1-\beta_1}(x,q)$ ($n \in \mathbb{N}$, $0 < \beta_1 < 1$). Later a slightly modified generating function method (MGFM) [15,16,17,34,36] has been established. The crux of this method is that it derives the very same solution, by starting directly from the wave equation (19), and arriving straightforwardly at the PDE for the output light wave, without making the detour via the RN equations. Notwithstanding this simplification, it remains a cumbersome task to investigate the properties of the Mathieu functions of fractional order, for which the coefficients of their Fourier series are not nearly as well tabulated as for the simpler periodic Mathieu functions (see e.g. [1]). In many instances, these coefficients have to be calculated and even on modern computers this remains a hard and timeconsuming job (see e.g. [68]). Just as in the case of normal incidence of the light, we shall pay close attention to the approximate and numerical solutions of the system (71) or (74) with boundary conditions (72).

In Section 6 a survey will be given of some approximate methods. One of these methods, i.e. the Nth order approximation method, will be considered in detail in Section 7. This method leads to a finite system of first order differential equations. The solution is then further reduced to a classical eigen-

value problem, which is clearly suited for numerical treatment. In the next Section, the results will be compared with the experimental data of Mayer [63] and Klein et al. [62]. Some considerations about the asymmetry of the diffraction spectra are also given and a comparison with Raman-Nath's elementary theory is made. Approximate methods due to Phariseau [66], and Blomme and Leroy [56], are discussed in Section 9. Furthermore, Phariseau's results are compared there with these obtained from the 1OA method for several values of ρ and Q.

NOMENCLATURE

We refer to the nomenclature given in Part I. New and additional symbols and abbreviations are :

$a = 2\varepsilon_r\lambda/\varepsilon_1\lambda^*$	factor of the term containing sin φ in the RN equations
$\mathbf{A}^{(k)}$	eigenvector associated with the eigenvalue s_k (column matrix with the $2N+1$ components)
C_k	real constant
h	height of the liquid column
$\mathbf{I}$	$(2N+1)\times(2N+1)$ unit matrix
$\mathbf{M}$	$(2N+1)\times(2N+1)$ Hermitian matrix
$\tilde{\mathbf{M}}$	$(M+N+1)\times(M+N+1)$ Hermitian matrix
s_k	k^{th} (real) eigenvalue of $\mathbf{M}$
β	parameter proportional to sin φ
$\rho_+ = \rho\,(1+\beta)$	multiple of the regime parameter
$\rho_- = \rho\,(1-\beta)$	multiple of the regime parameter
MNOA	M-N^{th} order approximation
NOA	N^{th} order approximation

6. Approximate methods in the case of oblique incidence of the light

6.1. *The approximate solution due to Brillouin-Debye*

Shortly after the discovery of the acousto-optic effect in 1932 by Debye and Sears in the USA and by Lucas and Biquard in France, Brillouin [57] and Debye [58] independently developed a theory based on the — at that time very fashionable — method of retarded potentials (see for instance [71]).

Starting from the wave equation (19) they put

$$E = E_o + E_1, \tag{76}$$

where E_1 is the perturbation of the initial electrical field E_o of the incident light beam. They obtain

$$(E_1)_{\pm} \approx \frac{\sin \frac{\pi L}{\lambda}(\cos\theta - \cos\varphi)}{\frac{\pi L}{\lambda}(\cos\theta - \cos\varphi)} \frac{\sin \frac{\pi h}{\lambda}(\sin\theta - \sin\varphi \pm \frac{\lambda}{\lambda^*})}{\frac{\pi h}{\lambda}(\sin\theta - \sin\varphi \pm \frac{\lambda}{\lambda^*})} \times e^{i(\omega \mp \omega^*)t} \quad (77)$$

where θ is the angle between the direction of observation and the z-axis (cf. Fig. 1) and h the height of the liquid column. This early approximation, although restrained to the amplitudes of orders +1 and -1, contains all the relevant information about the spectrum. Indeed, the complex time factor accounts for the Doppler shift $\mp\omega^*$; the remaining factors will allow to determine the directions of the light beams that produce the spectrum. In order to calculate these directions, we write the sine factors in (77) as follows

$$\underbrace{\frac{\sin \frac{\pi L}{2\lambda}(\theta^2 - \varphi^2)}{\frac{\pi L}{2\lambda}(\theta^2 - \varphi^2)}}_{A} \underbrace{\frac{\sin \frac{\pi h}{2\lambda}(\theta - \varphi \pm \frac{\lambda}{\lambda^*})}{\frac{\pi h}{2\lambda}(\theta - \varphi \pm \frac{\lambda}{\lambda^*})}}_{B_{\mp}}, \quad (78)$$

equating the sines of the angles with their arguments. This is allowed since in the experimental setup the angles θ and φ are always very small. For convenience, let us denote the first factor by A and the second one by $B_{\mp}$. They are represented schematically as functions of θ in Fig. 22. For decreasing

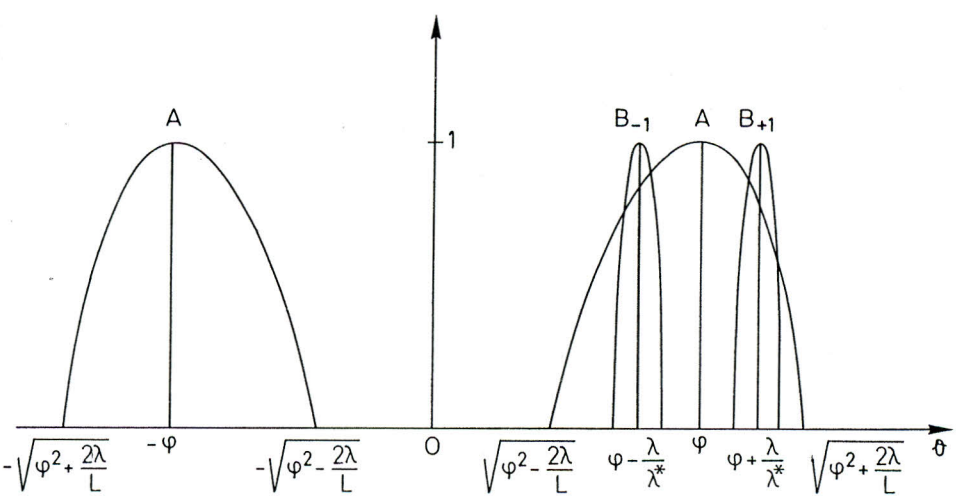

Fig. 22. — Schematic representation of the functions $A(\theta, \varphi)$ and $B_{\mp}(\theta, \varphi)$ as in (78) for varying θ.

values λ^* the maxima of $B_{\mp}$ separate, for increasing λ^* these maxima approach each other. For a suitable value of φ a superposition of the maxima of $B_{\mp}$ with the maximum of A, corresponding with the direction of the reflected light at angle $-\varphi$, may be obtained. This leads to $\varphi \pm \frac{\lambda}{\lambda^*} = -\varphi$, or

$$\varphi = \varphi_{BR}^{(\mp 1)} = \mp \frac{\lambda}{2\lambda^*}, \tag{79}$$

expressing that the highest intensities of the spectral orders ∓ 1 correspond with light incident at Bragg angles of orders ∓ 1. On the other hand, (78) reveals that $B_{\mp}$ reaches its maximum 1 for

$$\theta_{\pm 1} = \varphi \mp \frac{\lambda}{\lambda^*}, \tag{80}$$

giving the diffraction angles of the orders ± 1 (see also (4)). For these angles the amplitudes of the diffracted light beams are proportional to

$$A_{\pm 1} = \frac{\sin \frac{\pi L}{2\lambda^*}\left(\frac{\lambda}{\lambda^*} \mp 2\varphi\right)}{\frac{\pi L}{2\lambda^*}\left(\frac{\lambda}{\lambda^*} \mp 2\varphi\right)} \tag{81}$$

Substituting $\varphi = \varphi_{BR}^{(p)} = \frac{\lambda}{2\lambda^*}$ in (81) we quickly find $A_{+1} = 1$ and

$$A_{-1} = \frac{\sin \frac{\pi\lambda L}{\lambda^{*2}}}{\frac{\pi\lambda L}{\lambda^{*2}}} = \frac{\sin \frac{Q}{2}}{\frac{Q}{2}}, \tag{82}$$

where $Q = \frac{2\pi\lambda L}{\lambda^{*2}}$ is the Klein-Cook parameter (27). For $Q = \frac{\pi}{2}$ one obtains an asymmetry of 20% since $A_{-1}^2 = 0.8$. For increasing Q the intensity A_{-1}^2 of the line of order -1 decreases and will pass through a first zero for $Q = 2\pi$. After that the intensity A_{-1}^2 never exceeds 5% of the intensity A_{+1}^2 in order 1. Hence, $Q = 2\pi$ may be considered as a lower bound for the phenomena of selective reflection or Bragg reflection. This situation is illustrated in Fig. 23, where $\varphi = \varphi_{BR} = \varphi_{BR}^{(1)}$. Assuming that the order -1 is negligible, only the zeroth and first orders submerge. Since the first order angle θ_1 is given by $\theta_1 = \varphi_{BR} - \frac{\lambda}{\lambda^*} = \frac{\lambda}{2\lambda^*} = -\varphi_{BR}$, the first diffracted light beam behaves as if it were reflected at the wave fronts of the ultrasonic wave.

An interesting aspect of this early perturbation method due to Brillouin and Debye is that it accounts for Bragg reflections and that it leads to the condition

$$Q \gtrapprox 2\pi \text{ (or } Q \gg 1) \tag{83}$$

for Bragg reflection in terms of the Klein-Cook parameter Q which — incidentally — was introduced some thirty years later !

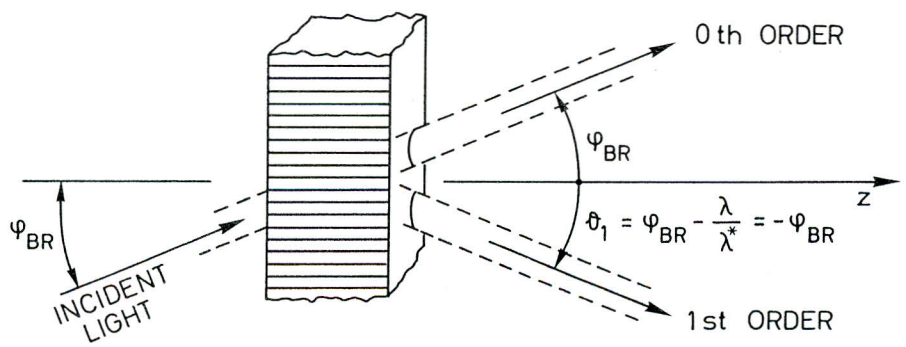

Fig. 23. — Single-order Bragg diffraction. Phenomenon of selective (or Bragg) reflection.

6.2. *Raman-Nath's elementary theory*

As in the case of normal incidence of the light, the simplest approximation is obtained by setting $\rho = 0$ in the infinite system (71) with boundary conditions (72). The solution in terms of the Bessel functions of integer order, was given in (29) and (30) :

$$\phi_n(\zeta) = J_n\left(\frac{\sin b\zeta}{b}\right) \exp(-inb\zeta) \ , \tag{84}$$

with

$$b = \frac{1}{2} a \sin \varphi \ . \tag{85}$$

At the boundary $z = L$ the intensities are

$$I_n = I_{-n} = J_n^2(v_\varphi) \tag{86}$$

with

$$v_\varphi = v \frac{\sin(Q\beta/4)}{Q\beta/4} \ . \tag{87}$$

The argument of the Bessel function is conveniently expressed in terms of Q and β. The symmetry of the diffraction pattern with respect to the zeroth order line is obvious from (86). In Fig. 24 the intensities I_0 and $I_{\pm 1}$ are shown versus β for $Q \ll 1$, namely for $Q = 0.1$, with $v = 1,2$ and 3. From (87) it is also clear that the intensities are symmetric with respect to $\beta = 0$.

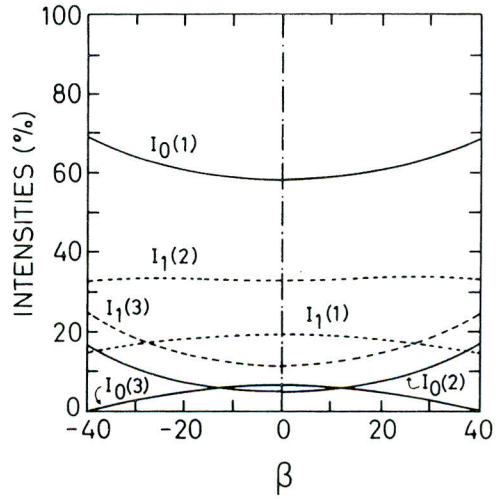

Fig. 24. — I_0, I_1 ($= I_{-1}$) versus β for $Q = 0.1$, and $\nu = 1$, $\nu = 2$, $\nu = 3$, calculated from the Bessel function expressions (86), $J_n^2(\nu_\varphi)$ ($n = 0,1$), with ν_φ given by (87). The curves for $I_n(\nu,\beta)$ ($n = 0, \pm 1$), computed with the NOA method ($I_{-1} \approx I_{+1}$) practically coincide with those of $J_n^2(\nu_\varphi)$.

6.3. *Perturbation methods*

In order to obtain an improvement of RN's elementary formula (84), two perturbation methods were developed by Plancke-Schuyten et al [67]. They come about naturally within the framework of the GFM as in [26,37] or the MGFM discussed in [15,16,17,34,35,36].

6.3.1. Series expansion in ρ

The amplitude is expressed as a series in ρ

$$\phi_n(\zeta) = \sum_{k=0}^{\infty} (i\rho)^k \phi_{nk}(\zeta) \ . \tag{88}$$

The first term ϕ_{n0} is precisely given by (84). However, the calculation to second order is rather cumbersome [67] and the result does not yield any relevant information about the intensity in the neighbourhood of a Bragg angle.

6.3.2. Double series expansion in ρ and a

The amplitude of the nth order line is now expressed as a double series

$$\phi_n(\zeta) = \sum_{k,l=0}^{\infty} i^{k+l} \rho^k (2a \sin\varphi)^l \phi_{n,kl}(\zeta) \ , \tag{89}$$

subject to the condition

$$(1-\varepsilon)\frac{\rho}{2a} < |\sin\varphi| < (1+\varepsilon)\frac{\rho}{2a}\ ,\ 0<\varepsilon \ll 1. \tag{90}$$

A straightforward but lenghty calculation leads to the expression for the intensity of the nth order line at $z = L$

$$I_n(v,\varphi) = J_n^2(v) + \frac{1}{24}a\sin\varphi\, v^3(2\rho n - 2a\sin\varphi)\, J_n(v)\, J_n'(v)$$
$$-\frac{1}{720}\rho^2 v^2\left[(7n^2-9v^2)\, J_n^2(v) + (16n^2-3)vJ_n(v)\, J_n'(v) - 5v^2 J_n'^2(v)\right],$$
$$n = 0, \pm 1, \pm 2, \ldots \tag{91}$$

where $J_n'(v) = \frac{dJ_n(\zeta)}{d\zeta}\Big|_{\zeta=v}$.

As a matter of verification, observe that the second term vanishes for $\varphi = 0$. Hence, expression (91) reduces to (44), obtained for $\rho \ll 1$ in the case of normal incidence of the light. Furthermore, the second term in (91) accounts for the *asymmetry* of the spectrum with respect to the zeroth order line. To investigate the intensity I_n as a function of the angle of incidence φ, we take the derivative of I_n with respect to $\sin\varphi$. We obtain with $\cos\varphi \approx 1$,

$$\frac{dI_n(v,\varphi)}{d\sin\varphi} = \frac{1}{12}av^3(n\rho - 2a\sin\varphi)\, J_n(v)\, J_n'(v)\ , \tag{92}$$

which equals zero for $\sin\varphi = \frac{n\rho}{2a}$, reestablishing the Bragg relation (75). This comfirms that $I_n(v,\varphi)$ reaches an extremum for $\varphi = \varphi_{BR}^{(n)}$. For a detailed discussion of those extrema we refer to the original paper by Plancke-Schuyten et al [67].

6.4. *The Nth order approximation method (NOA method)*

As we mentioned in the Introduction, the success of the NOA method in the case of normal incidence of the light led us to generalize this method to the case of oblique incidence of the light. Furthermore, as before, it will be the basis for the numerical treatment of the problem. In order to obtain a solution within the NOA, we set in the RN system (74), $\phi_{\pm(N+1)} = \phi_{\pm(N+2)} = \ldots = 0$. Physically this means that we neglect all energy in the diffraction orders higher than N. The infinite system (74) is thus truncated to a system with $2N+1$ equations,

$$2\frac{d\phi_{-N}}{d\zeta} + \phi_{-(N-1)} = -i\rho\, N(-N+\beta)\,\phi_{-N_1},$$

$$2\frac{d\phi_n}{d\zeta} - \phi_{n-1} + \phi_{n+1} = i\rho n\,(n+\beta)\,\phi_n\,,\ n = 0, \pm 1, \pm 2,\ldots,\pm(N-1), \tag{93}$$

$$2\frac{d\phi_N}{d\zeta} - \phi_{N-1} = i\rho\, N(N+\beta)\phi_N\ .$$

The coupled amplitudes ϕ_0, $\phi_{\pm 1}$, ..., $\phi_{\pm N}$ must satisfy the boundary conditions

$$\phi_n(0)=\delta_{n0}\ ,\ n=0,\pm 1,\pm 2,\ldots,\pm N. \tag{94}$$

In the case of oblique incidence of the light this method was introduced by Nagabhushana Rao [65] for $N = 1$ and it led to analytic expressions for the intensities of orders $0,\pm 1$. A derivation of those formulae, using the method discussed in the next Section will be given in Appendix C.

7. Solution of the truncated RN system (93)-(94)

Assuming the following form of the solution:

$$\phi_n(\zeta)=A_n \exp\left(\frac{1}{2}is\zeta\right)\ ,\ n=0,\pm 1,\ldots,\pm N, \tag{95}$$

and substituting it into the system (93), gives rise to a system of $2N + 1$ linear homogeneous equations for A_0, $A_{\pm 1}$, ..., $A_{\pm N}$. Hence, the integration of system(93) is reduced to solving an eigenvalue problem

$$(\mathbf{M}-s\mathbf{I})\ \cdot\ \mathbf{A}=\mathbf{0}, \tag{96}$$

where $\mathbf{I}$ is the $2N + 1$ by $2N + 1$ identity matrix, $\mathbf{A}^T= (A_{-N} \ldots A_{-2}\ A_{-1}\ A_0\ A_1\ A_2 \ldots A_N)$ and where the $2N + 1$ by $2N + 1$ Hermitian matrix $\mathbf{M}$ is explicitly given by

$$\begin{bmatrix}
\rho\, N(N-\beta) & i & 0 & \ldots & . & . & . & \ldots & . & . & 0 \\
-i & \rho(N-1)(N-1-\beta) & i & \ldots & . & . & . & \ldots & . & . & 0 \\
. & . & . & \ldots & . & . & . & \ldots & . & . & . \\
. & . & . & \ldots & . & . & . & \ldots & . & . & . \\
. & . & . & \ldots & . & . & . & \ldots & . & . & . \\
0 & . & . & \ldots & \rho(1-\beta) & i & 0 & \ldots & . & . & 0 \\
0 & . & . & \ldots & -i & 0 & i & \ldots & . & . & 0 \\
0 & . & . & \ldots & 0 & -i & \rho(1+\beta) & \ldots & . & . & 0 \\
. & . & . & \ldots & . & . & . & \ldots & . & . & . \\
. & . & . & \ldots & . & . & . & \ldots & . & . & . \\
. & . & . & \ldots & . & . & . & \ldots & . & . & . \\
0 & . & . & \ldots & . & . & . & \ldots & -i & \rho(N-1)(N-1+\beta) & i \\
0 & . & . & \ldots & . & . & . & \ldots & 0 & -i & \rho N(N+\beta)
\end{bmatrix} \tag{97}$$

Since the matrix is Hermitian its $2N + 1$ eigenvalues are real [11]. For a nonzero vector solution $\mathbf{A}$ the eigenvalues s must be the $2N + 1$ roots of the characteristic equation

$$\det(\mathbf{M}-s\mathbf{I}) = 0. \tag{98}$$

Next, the eigenvector $\mathbf{A}^{(k)}$ with $\mathbf{A}^{(k)T} = (A_{-N}^{(k)} \ldots A_{-1}^{(k)} A_0^{(k)} A_1^{(k)} \ldots A_N^{(k)})$ associated with the eigenvalue s_k ($k = 1, 2, \ldots, 2N + 1$) can be determined from the linear homogeneous system

$$(\mathbf{M}-s_k\mathbf{I}) \cdot \mathbf{A}^{(k)} = \mathbf{0}. \tag{99}$$

The general solution of the linear difference-differential system (93) may then be written as

$$\phi_n(\zeta) = \sum_{k=1}^{2N+1} C_k A_n^{(k)} \exp\left(\frac{1}{2} i s_k \zeta\right), \quad n = 0, \pm 1, \ldots, \pm N. \tag{100}$$

Taking into account the boundary conditions (94), the $2N + 1$ real constants C_k follow from

$$\sum_{k=1}^{2N+1} C_k A_n^{(k)} = \delta_{n0}, \quad n = 0, \pm 1, \ldots, \pm N. \tag{101}$$

Finally, one calculates the intensities at $z = L$, yielding

$$I_n(v) = |\phi_n(v)|^2 = \delta_{n0} - 4 \sum_{\substack{k,l=1 \\ k<l}}^{2N+1} C_k C_l A_n^{(k)} \overline{A_n^{(l)}} \sin^2 (s_k - s_l) \frac{v}{4}, \quad n = 0, \pm 1, \ldots, \pm N. \tag{102}$$

The characteristic equation (98) of degree $2N + 1$ in s, can only be solved analytically for $N = 1$. Thus, only in this simplest case an explicit analytical expression for the intensities can and has been obtained [65]. For $N > 1$ the problem has to be treated numerically in the following steps:

(i) determine the eigenvalues and the eigenvectors of the matrix $\mathbf{M}$ by solving (98) and (99);
(ii) solve the linear system (101) for C_k;
(iii) substitute these results into (102).

Various cases have been treated this way and the results were very satisfactory as will be clear form the discussion in the next Section.

8. Numerical results and discussion

8.1. *Comparison with Mayer's experiments*

In Fig. 25 we compare $I_0(\varphi)$ and $I_{-1}(\varphi)$, obtained from the NOA method for $N = 7$), with the experimental results of Mayer [63] for $Q = 4.28$. The

fitting of both curves is clearly very good. A similar result for $Q = 8.36$ is shown in Fig. 26. The purpose of Mayer's experiments was to exhibit the deviation from RN's elementary theory (cf. Subsection 6.2, Eqs. (86) and (87)), the latter leading to curves for e.g. the intensities I_0 and I_{-1}, which are symmetric with respect to $\varphi = 0$ (i.e. $\beta = 0$). This difference is confirmed by the results from the NOA method. Indeed, it is obvious from Figs. 25 and 26 that the intensities I_{-1} are no longer symmetric with respect to $\varphi = 0$, but that there is a symmetry with respect to the corresponding Bragg angle $\varphi_{BR}^{(-1)}$. This property is not restricted to the intensities of order –1, but follows from the exact theory by Plancke-Schuyten and Mertens [68] where it is shown for arbitrary n. In general, one has $I_n(v\,;\varphi^{(n-a)}) = I_n(v\,;\varphi^{(n+a)})$ ($n \in \mathbf{Z}$, $a \in \mathbf{R}$, with $\varphi^{(n)} = \varphi_{BR}^{(n)}$). Of course one should have a symmetry of I_0 with respect to $\varphi = 0$, but the curves in Figs. 25 and 26 are totally different from those given by Eq. (86) for $n = 0$ (compare with Figs. 3 and 4 in [63]), the latter being only valid for $Q \ll 1$.

Similar results were also obtained recently by Leroy and Blomme by a so-called MNOA method [56] to be discussed in Section 9.1.

8.2. *Comparison with Klein's results*

Now we compare I_0 and I_{-1} versus β, calculated by using the NOA method (with N=7, although N=5 suffices for all values considered) with the experimental data obtained by Klein et al [62]. The comparison is carried out for different combinations of the parameters Q and v. The results are shown in Fig. 27 (Q=0.57), Fig. 28 (Q=2.25), Fig. 29 (Q=3.74), Fig. 30 (Q=6.28) and Fig. 31 (Q=9.3). In each of these figures two values of v were selected : $v = 2$ (figures on the left) and $v = 3$ (figures on the right). There is excellent agreement with the measured values. Our curves fit the data even better than the curves calculated by Klein et al [62], using a direct numerical integration algorithm divised by Klein et al [61].

Furthermore, our numerical integration method results in accurate plots for even larger values of $|\beta|$ and it has the advantage that it is based on analytical expressions for the intensities in terms of sums of squared sine functions (see (102)). The unknown quantities in these expressions are the eigenvalues and the components of the eigenvectors of the Hermitian matrix (97) and the constants C_k follow readily from solving of a linear system of algebraic equations. For all of these steps, highly accurate computer algorithms are readily available.

Looking at the Figs. 27 through 31, the following properties — well-known from the exact theory [15,16,17,68] — are confirmed :

— Intensity I_{-1} reaches an extremum at the first order Bragg angle $\varphi_{BR}^{(-1)}$, i.e. $\beta = 1$;

— Intensity distributions of I_{-1} are symmetric about $\varphi_{BR}^{(-1)}$.

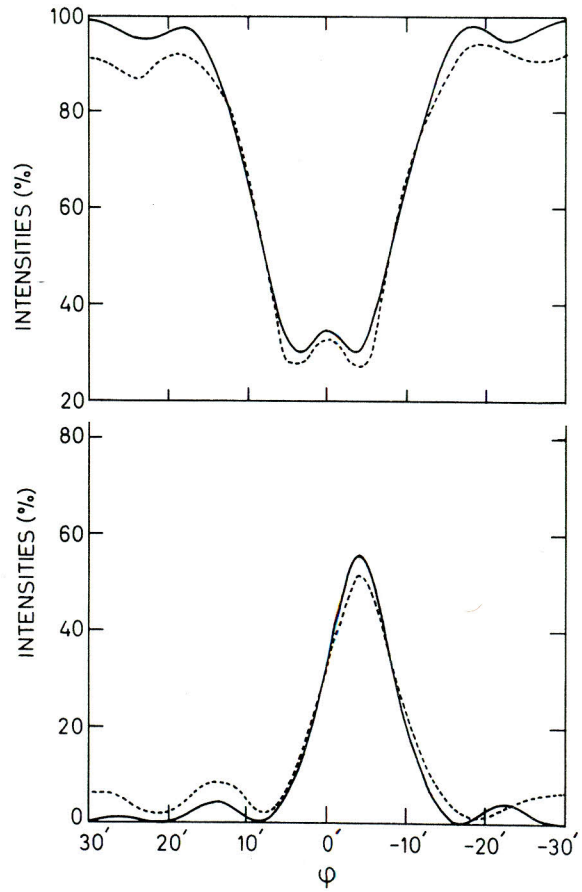

Fig. 25. — I_0 (top) and I_{-1} (bottom) versus φ. Mayer's experiments [63] (dotted line) ; NOA method (full line), for $Q = 4.28$.

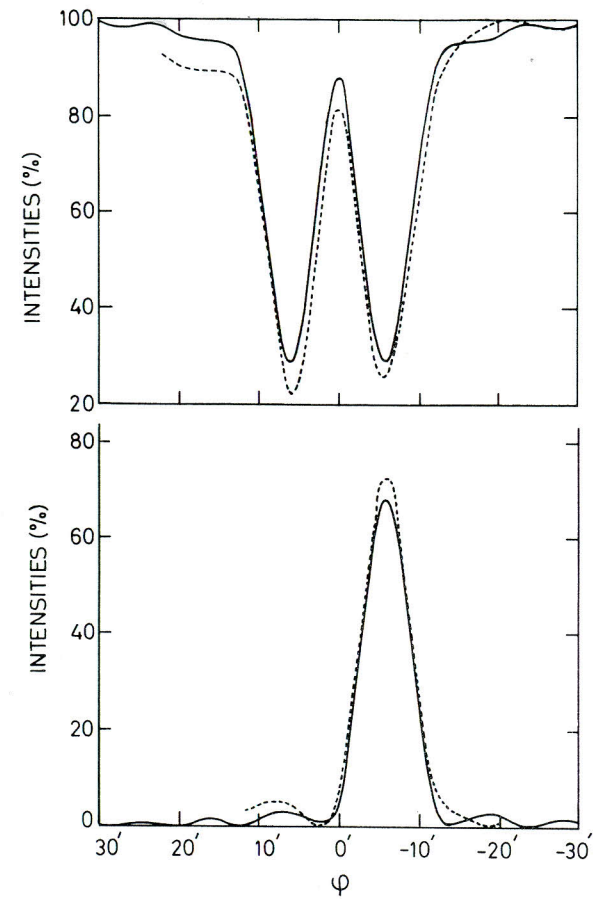

Fig. 26. — I_0 (top) and I_{-1} (bottom) versus φ. Mayer's experiments [63] (dotted line) ; NOA method (full line), for $Q = 8.36$.

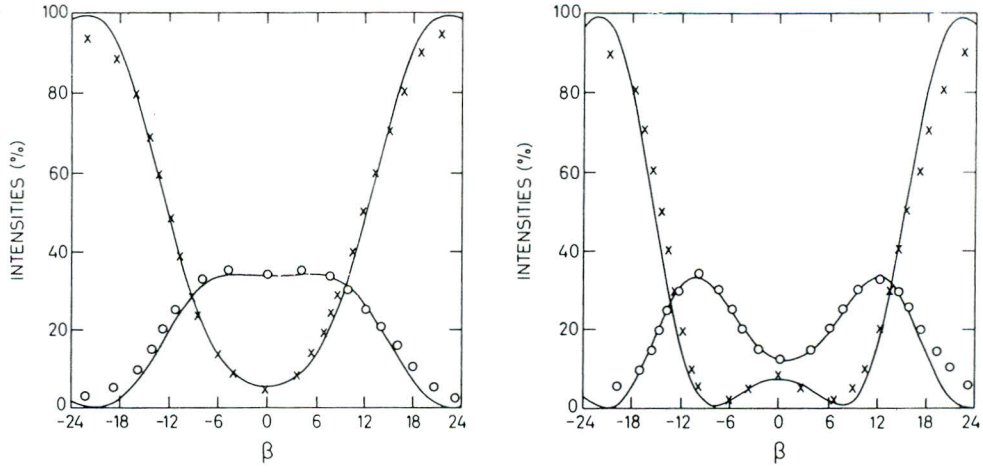

Fig. 27. — I_0 and I_{-1} versus β for $Q = 0.57$, $\nu = 2$ (left) and $\nu = 3$ (right). NOA method (full line) ; experiments of Klein et al [62] (I_0 : ×××, I_{-1} : ○○○).

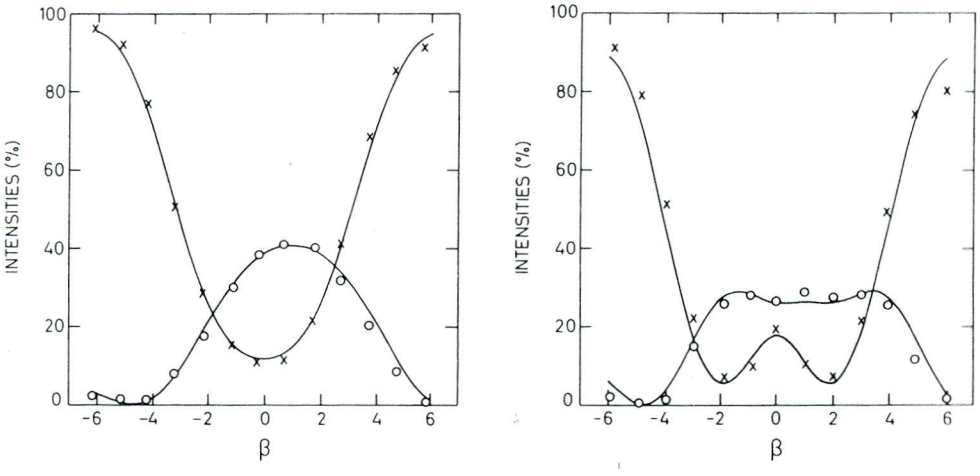

Fig. 28. — As in Fig. 27, but for $Q = 2.25$.

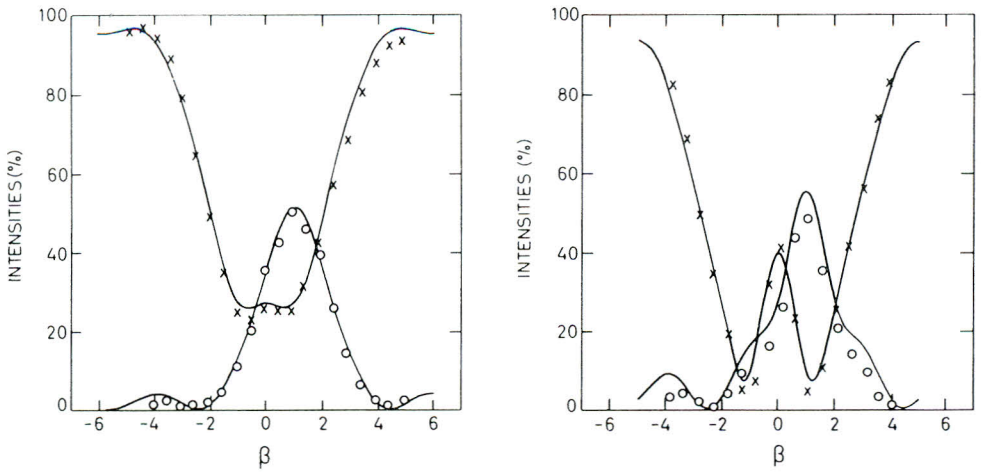

Fig. 29. — As in Fig. 27, but for $Q = 3.74$.

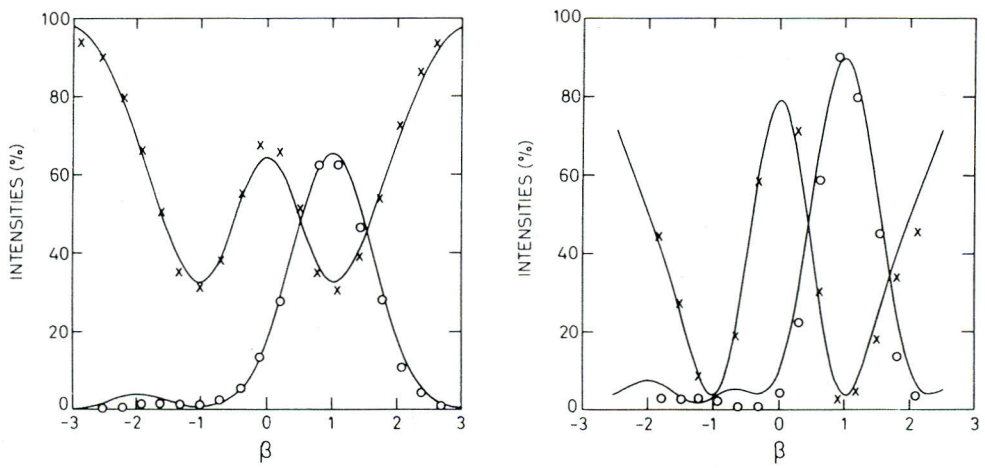

Fig. 30. — As in Fig. 27, but for $Q = 6.28$.

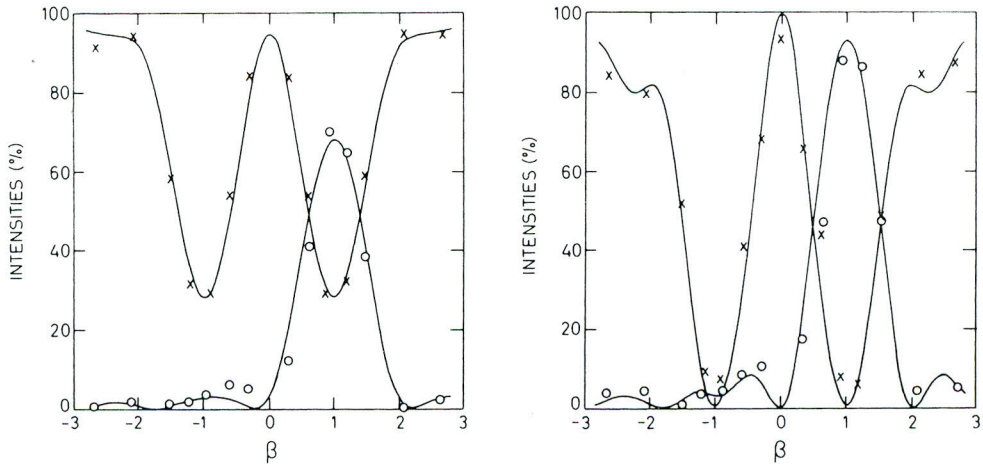

Fig. 31. — As in Fig. 27, but for $Q = 9.3$.

From our computer calculations it is clear that for $Q \gg 1$ (we took $Q = 9.3$), Bragg reflection of the light is a dominant effect, although, for certain values of β the intensities of orders +2 and –2 are not negligible.

8.3. *Asymmetry of the spectrum*

Besides comparing with experiments, we have also calculated the intensities I_0, $I_{\pm 1}$ and $I_{\pm 2}$ versus v, for $Q = 2.25$ with $\beta = 1$ (Fig. 32) and $\beta = 2$ (Fig. 33), showing clearly the asymmetry of the spectrum with respect to the zeroth order. Up to $v = 10$, it suffices to take $N = 5$ and even $N = 4$ would have produced excellent agreement with the theoretical prediction.

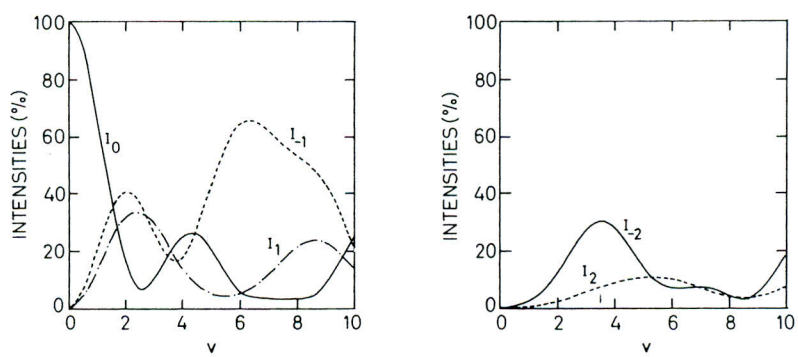

Fig. 32. — I_0, I_1, I_{-1} (left) and I_2, I_{-2} (right) for $Q = 2.25$ and $\beta = 1$, calculated with the NOA method.

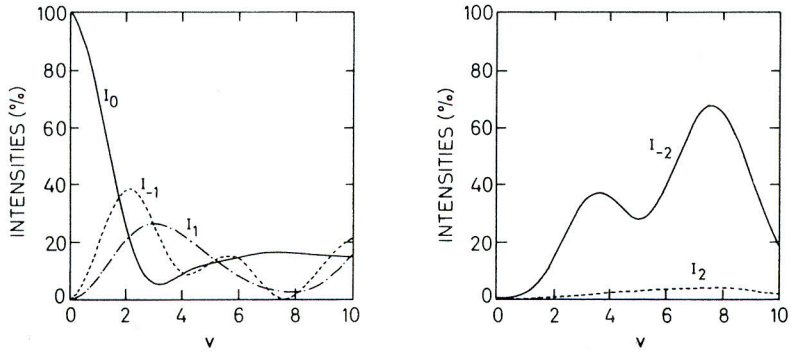

Fig. 33. — As in Fig. 32, but for $\beta = 2$.

8.4. *The elementary RN theory and the NOA method*

Finally, we have computed I_0 and $I_{\pm 1}$ versus β for $Q \ll 1$, namely for $Q = 0.1$, with $v = 1$, $v = 2$ and $v = 3$ using the NOA method ($N = 6$). Compared with the formulae from the elementary RN theory (see (86) and (87)), we get practically the same results (Fig. 24). In this case the symmetry of the diffraction pattern is also shown.

9. **Other analogous approximate methods**

9.1. *The MNOA method due to Blomme and Leroy*

Like the NOA method, the MNOA method is based on a truncation of Raman-Nath equations. The main difference is in the way the asymmetry of the spectra is dealt with. Indeed, in certain experimental setups (using oblique incidence of the light) the number of 'negative' orders is different from the number of 'positive' orders, thus inducing asymmetry in the spectrum (cf. Fig. 2a). To account for this, Blomme and Leroy [56] developed their so-called MNOA method. They assume that only M negative and N positive orders are present in the diffraction spectrum. Therefore only the amplitudes ϕ_{-M}, ..., ϕ_{-1}, ϕ_0, ϕ_1, ..., ϕ_N, with $M, N \in \mathbb{N}$ and $M \leq N$ ($\varphi > 0$) need to be considered. Adhering to a solution of the form (95) with ($n = -M, ..., -1, 0, 1, ..., N$) leads to an eigenvalue problem with matrix $\tilde{\mathbf{M}}$ given by

$$\begin{bmatrix} -\rho M(-M+\beta) & i & 0 & \dots & 0 & 0 & 0 & \dots & 0 & 0 & 0 \\ -i & -\rho(M-1)(-M+1+\beta) & i & \dots & 0 & 0 & 0 & \dots & 0 & 0 & 0 \\ \cdot & \cdot & \cdot & \dots & \cdot & \cdot & \cdot & \dots & \cdot & \cdot & \cdot \\ \cdot & \cdot & \cdot & \dots & \cdot & \cdot & \cdot & \dots & \cdot & \cdot & \cdot \\ \cdot & \cdot & \cdot & \dots & \cdot & \cdot & \cdot & \dots & \cdot & \cdot & \cdot \\ 0 & 0 & 0 & \dots & -i & 0 & i & \dots & 0 & 0 & 0 \\ \cdot & \cdot & \cdot & \dots & \cdot & \cdot & \cdot & \dots & \cdot & \cdot & \cdot \\ \cdot & \cdot & \cdot & \dots & \cdot & \cdot & \cdot & \dots & \cdot & \cdot & \cdot \\ \cdot & \cdot & \cdot & \dots & \cdot & \cdot & \cdot & \dots & \cdot & \cdot & \cdot \\ 0 & 0 & 0 & \dots & 0 & 0 & 0 & \dots & -i & \rho(N-1)(N-1+\beta) & i \\ 0 & 0 & 0 & \dots & 0 & 0 & 0 & \dots & 0 & -i & \rho N(N+\beta) \end{bmatrix} \tag{103}$$

The $(M + N + 1) \times (M + N + 1)$ matrix $\tilde{\mathbf{M}}$ is still Hermitian, so its $R = M + N + 1$ eigenvalues $s_1, s_2, \dots, s_R$ are all real. Denoting the eigenvector associated with the eigenvalue s_k by $\mathbf{A}^{(k)}$, where $\mathbf{A}^{(k)\,T} = (A^{(k)}_{-M} \dots A^{(k)}_{-1}\ A^{(k)}_0\ A^{(k)}_1 \dots A^{(k)}_N)$, the amplitudes may be written as,

$$\phi_n(\zeta) = \sum_{k=1}^{R} C_k A^{(k)}_n \exp\left(\frac{1}{2} i s_k \zeta\right), \; R = M + N + 1, \; n = -M, \dots, -1, 0, 1, \dots, N. \tag{104}$$

The determination of the constants C_k and the calculation of the intensities is analogous with the NOA case in Section 7. The MNOA method is advantageous when the numbers M and N are known *a priori*, i.e. when an experimentally obtained spectrum has to be analyzed theoretically. If no information about the spectrum is known yet, then it is advisable to use the NOA-method where the number of orders N is determined by the computer. In this case the algorithm will select a value of N such that all the nonvanishing orders (negative and positive) are taken into account.

9.2. *Special cases*

Phariseau [66] was the first to introduce the MNOA method for special cases. He considered $M = 0$, $N = 1$, and $M = 1$, $N = 2$ and took angles of incidence in the neighbourhood of a Bragg angle. Phariseau's formulae for the case $M = 1$, $N = 2$ are only approximate. The MNOA method applied in the near Bragg region, was rewritten in terms of Feynman diagrams by Poon and Korpel. This led to explicit solutions for $M = 1$, $N = 2$ [69,70]. An exact 4th-order solution for $M = 1$, $N = 2$ was given by Blomme and Leroy [55].

Now, we derive Phariseau's results for $M = 0$, $N = 1$ using the eigenvalue problem. From the Brillouin-Debye approximate solution (Subsection 6.1), we

learned that provided $Q \gtrapprox 2\pi$, the intensity I_{-1} may be ignored for $\varphi \approx \varphi_{BR}^{(1)}$, so that only the orders 0 and + 1 are relevant. The truncated RN system in this approximation (i.e. $\beta \approx -1$, $M = 0$, $N = 1$) reads

$$2\frac{d\phi_0}{d\zeta} + \phi_1 = 0, \tag{105}$$

$$2\frac{d\phi_1}{d\zeta} - \phi_0 = i\rho_+ \phi_1$$

with $\rho_+ = \rho\,(\beta + 1)$. The boundary conditions still are

$$\phi_n\,(0) = \delta_{n0}\ \ , n = 0,1. \tag{106}$$

Projecting a solution of the form

$$\phi_n = A_n \exp\left(\frac{1}{2} is\zeta\right)\ , n = 0,1, \tag{107}$$

we have

$$\tilde{\mathbf{M}} = \begin{pmatrix} 0 & i \\ -i & \rho_+ \end{pmatrix}. \tag{108}$$

The eigenvalues of $\tilde{\mathbf{M}}$ are determined by

$$\det\,(\tilde{\mathbf{M}} - s\,\mathbf{I}) = \begin{vmatrix} -s & i \\ -i & \rho_+ - s \end{vmatrix} = 0 \tag{109}$$

or

$$s^2 - \rho_+ s - 1 = 0. \tag{110}$$

Translated in Phariseau's notation we thus have

$$s^2 - 4\sigma s - 1 = 0, \tag{111}$$

where

$$\rho_+ = 4\sigma. \tag{112}$$

The eigenvalues then are

$$s_1 = 2\sigma + \sqrt{4\sigma^2 + 1}\ \ , s_2 = 2\sigma - \sqrt{4\sigma^2 + 1}\ . \tag{113}$$

The components of the eigenvectors must satisfy

$$(\tilde{\mathbf{M}} - s_k\mathbf{I}) \cdot \mathbf{A}^{(k)} = \mathbf{0}\ \ ,\ \ k = 1,2. \tag{114}$$

Hence, for $k = 1$ we ought to solve

$$\begin{aligned} -s_1 A_0^{(1)} + i A_1^{(1)} &= 0, \\ -i A_0^{(1)} + (4\sigma - s_1) A_1^{(1)} &= 0. \end{aligned} \tag{115}$$

Up to a proportionality factor the solution is

$$A_0^{(1)} = 1 \ , \ A_1^{(1)} = -is_1 \ . \tag{116}$$

For $k = 2$ we obtain

$$A_0^{(2)} = 1 \ , \ A_1^{(2)} = -is_2 \ . \tag{117}$$

The amplitudes are then expressed as

$$\phi_0 = C_1 \exp\left(\frac{1}{2} is_1\zeta\right) + C_2 \exp\left(\frac{1}{2} is_2\zeta\right) , \tag{118}$$

$$\phi_1 = -i\, C_1 s_1 \exp\left(\frac{1}{2} is_1\zeta\right) - i\, C_2 s_2 \exp\left(\frac{1}{2} is_2\zeta\right) .$$

The constants C_1 and C_2 are the solutions of

$$C_1 + C_2 = 1 \ , \ s_1 C_1 + s_2 C_2 = 0, \tag{119}$$

which in turn follow from the boundary conditions. Substituting

$$C_1 = -\frac{s_2}{s_1 - s_2} \ , \ C_2 = -\frac{s_1}{s_1 - s_2} \tag{120}$$

into (118) and calculating the intensities at $z = L$ ($\zeta = v$), leads to

$$I_0 = 1 + \frac{4s_1 s_2}{(s_1 - s_2)^2} \sin^2 \frac{1}{4} (s_1 - s_2)v, \tag{121}$$

$$I_1 = 4\left(\frac{s_1 s_2}{s_1 - s_2}\right)^2 \sin^2 \frac{1}{4} (s_1 - s_2)v. \tag{122}$$

Since $s_1 s_2 = -1$ and $s_1 - s_2 = 2\sqrt{4\sigma^2 + 1}$, we finally get

$$I_0 = 1 - \frac{1}{4\sigma^2 + 1} \sin^2\left(\sqrt{4\sigma^2 + 1}\,\frac{v}{2}\right) , \tag{123}$$

$$I_1 = \frac{1}{4\sigma^2 + 1} \sin^2\left(\sqrt{4\sigma^2 + 1}\,\frac{v}{2}\right) . \tag{124}$$

These are Phariseau's well-known results. For perfect Bragg diffraction $\varphi = \varphi_{BR}^{(1)}$, so $\beta = -1$ and $\sigma = 0$, the formulae (123)-(124) simplify into

$$I_0 = \cos^2 \frac{v}{2} , \tag{125}$$

$$I_1 = \sin^2 \frac{v}{2} . \tag{126}$$

Here we encounter the rather curious fact that the intensities I_0 and I_1 are independent of ρ or Q.

9.3. *Some numerical results*

To conclude this Section we comment on some numerical calculations. In Fig. 34 the intensities I_0 (figure on the left) and I_1 and I_{-1} (figure on the right) versus v are shown. The various curves are calculated for Bragg incidence ($\beta = -1$) with Phariseau's formulae (125), (126) and with the 1OA method (see : Nagabhushana Rao's formulae (C19), (C20), (C21) in Appendix C). Both sets of theoretical results are compared for $Q = 9.3$ with experimental data obtained by Klein et al [62]. The fitting of the 1OA curves with the experimental points is excellent. Unfortunately the experimental data are restricted to the domain $v \in [0,4]$. In the same region for v there is a rather good agreement with Phariseau's results, but it fails beyond $v \approx 5$, due to the fact, that from thereon I_{-1} is no longer negligible. As a matter of fact, I_{-1} may in some cases take as much as 70% of the incident energy. Hence, we can conclude that

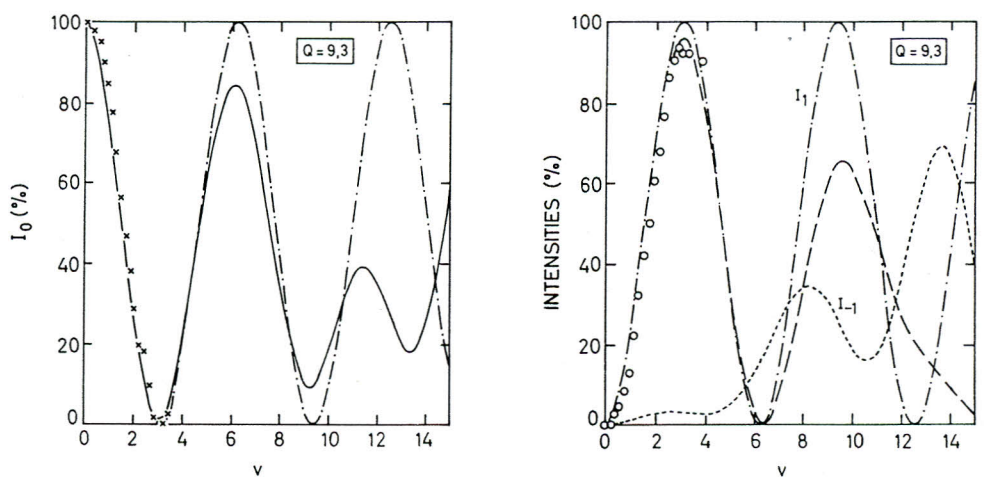

Fig. 34. — I_0 versus v (left), for $Q = 9.3$ and $\beta = -1$ calculated from Phariseau's formula (125) (—·—·—) and from Nagabhushana Rao's formula (C20) (———) compared with experimental data of Klein et al (×××) ; I_1 versus v (right) for $Q = 9.3$ and $\beta = -1$ calculated from Phariseau's formula (126) (—·—·—) and from (C21) (— — —) compared with experimental results of Klein et al (ooo) and I_{-1} versus v for the same values of Q and β from (C19).

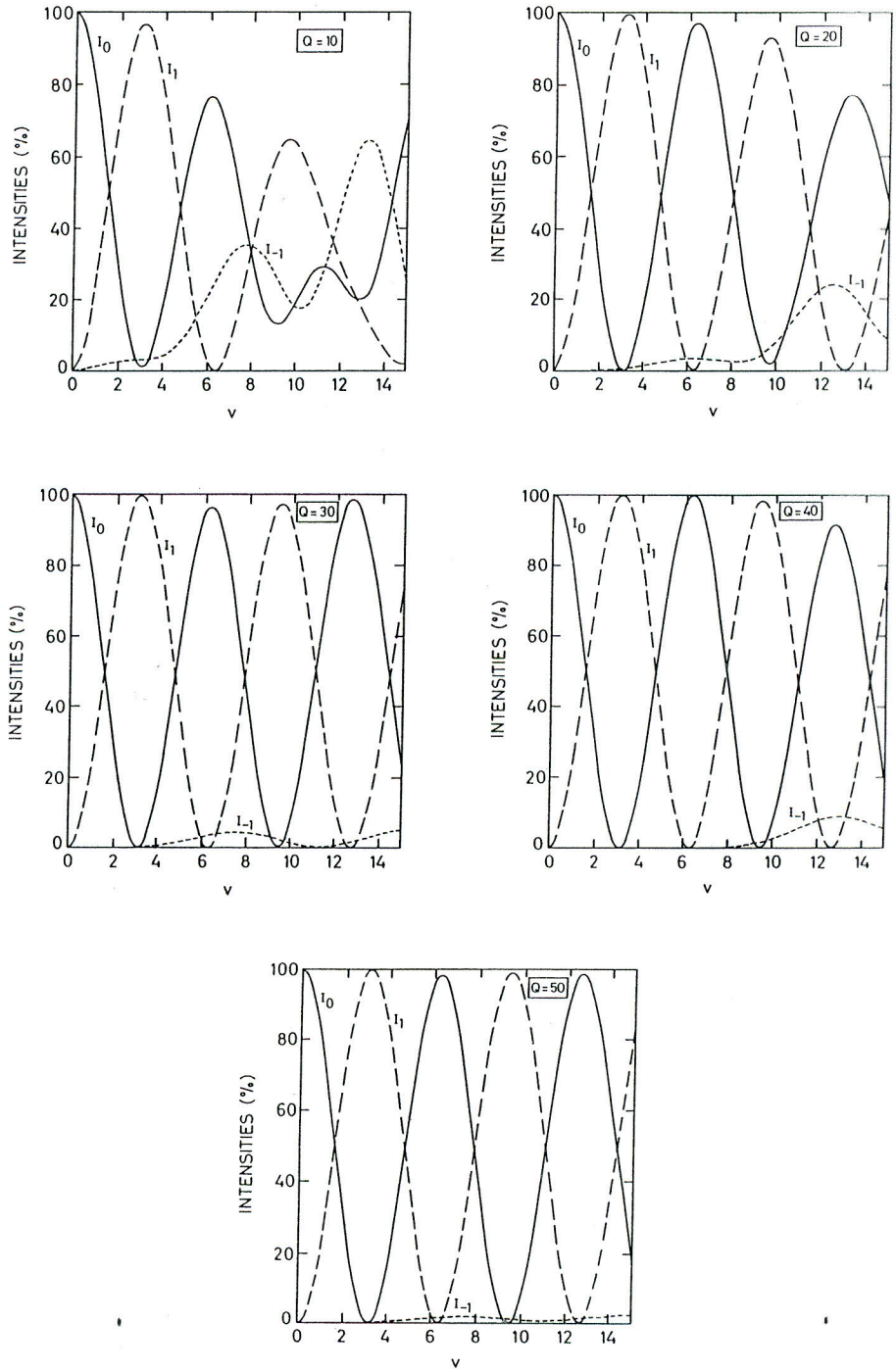

Fig. 35. — I_0 (———), I_1 (— — —) and I_{-1} (- - -) versus v respectively calculated from (C20), (C21), (C19) at Bragg incidence ($\beta = -1$) for $Q = 10$, 20, 30, 40 and 50.

for $Q = 9.3$ there is only "pure" Bragg reflection up to $v \approx 5$. In Fig. 35 we represent the curves for I_0, I_{+1} and I_{-1} versus v, calculated with the 1OA method at Bragg incidence (matching (C19), (C20) and (C21)), for increasing values of the Klein-Cook parameter, namely $Q = 10,20,30,40$ and 50. We ascertain that the larger the value of Q, the better the condition for "pure" Bragg reflection is satisfied. This is because the intensities I_{-1} decrease with higher values of v. Incidentally, the deviation of the curves for I_0 and I_1 from the squared cosine and sine functions (Phariseau's theory) becomes small with larger Q. In passing, we note that the use of the MNOA method is not appropriate for those values of v where I_{-1} is not evanescent. Finally, in Fig. 36 we again show I_0, I_{+1} and I_{-1} versus v, but now computed from

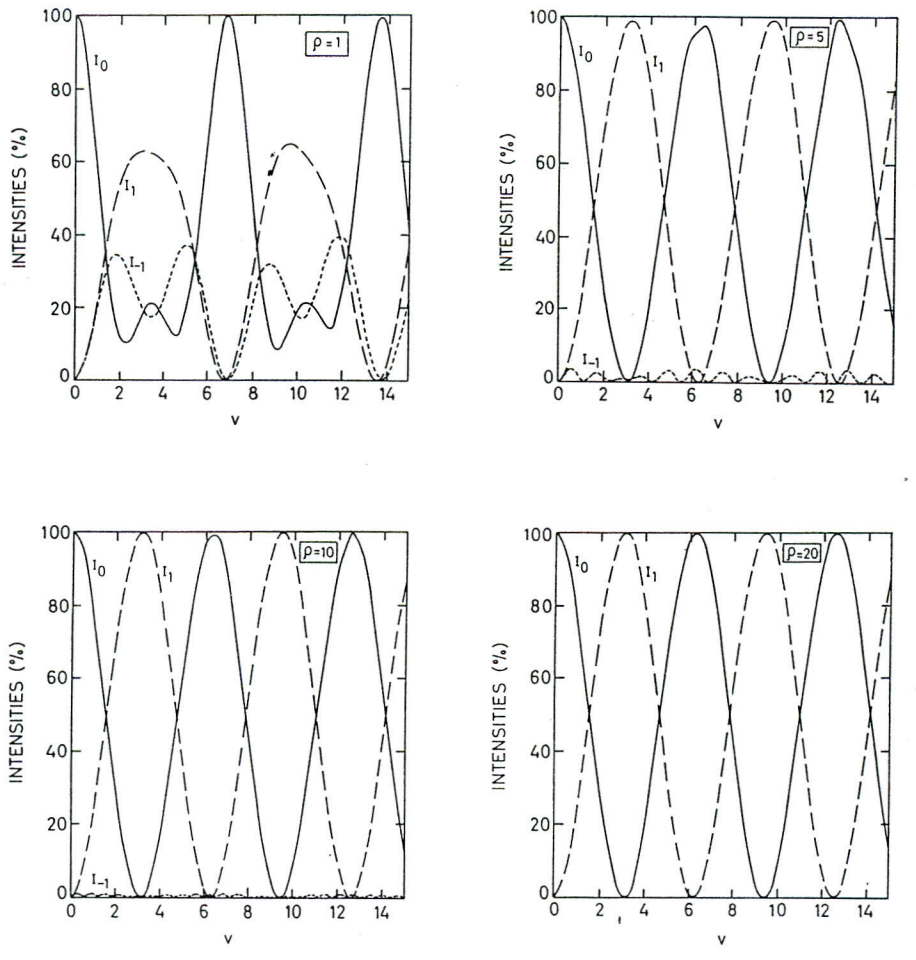

Fig. 36. — I_0 (———), I_1 (— — —) and I_{-1} (- - -) versus v respectively calculated from (C20), (C21), (C19) at Bragg incidence ($\beta = -1$) for $\rho = 1$, 5, 10 and 20.

Nagabhushana Rao's formulae (C19), (C20) and (C21) at Bragg incidence ($\beta = -1$) for increasing values of the regime parameter, i.e. $\rho = 1,5,10$ and 20. Similar calculations were performed for $\rho = 30,40$ and 50, but soon it became clear that the results were identical with those for $\rho = 20$. The curves for $\rho = 1$ do not illustrate Bragg reflection very well. Observe that in this case most values of I_{-1} are too large, and that second order intensities are not negligible. But for $\rho \geq 5$, the calculated values of I_{-1} keep decreasing ; practically vanishing for $\rho = 20$. Furthermore, I_0 and I_{+1} are nearly represented by Phariseau's formulae (125) and (126). This shows that for $\rho \geq 5$ there is near Bragg reflection, whereas for $\rho \geq 20$ we have "pure" Bragg reflection for which only the zeroth and first orders submerge.

Hence, it is clear that both the Klein-Cook parameter Q and the regime parameter ρ are relevant for determining the conditions of Bragg reflection.

APPENDIX C

An example of the use of the eigenvalue problem developed in Section 7

We take $N = 1$, which will lead to an analytical solution of the problem. The truncated system (93) becomes

$$2\frac{d\phi_{-1}}{d\zeta} + \phi_0 = i\rho_-\phi_{-1} ,$$

$$2\frac{d\phi_0}{d\zeta} - \phi_{-1} + \phi_1 = 0 , \tag{C1}$$

$$2\frac{d\phi_1}{d\zeta} - \phi_0 = i\rho_+\phi_1 ,$$

with boundary conditions

$$\phi_0(0) = 1 \ , \ \phi_{\pm 1}(0) = 0 , \tag{C2}$$

wherein

$$\rho_- = \rho(1 - \beta) , \tag{C3}$$

$$\rho_+ = \rho(1+\beta) . \tag{C4}$$

We assume a solution of the form

$$\phi_n = A_n \exp\left(\frac{1}{2} is\zeta\right) , \quad n = -1,0,+1. \tag{C5}$$

Upon substitution in system (C1) we obtain the following system of linear homogeneous equations

$$\begin{aligned} (\rho_- - s)\, A_{-1} + i\, A_0 &= 0, \\ -i\, A_{-1} - s\, A_0 + i\, A_1 &= 0, \\ -i\, A_0 + (\rho_+ - s)\, A_1 &= 0, \end{aligned} \tag{C6}$$

leading to the characteristic equation

$$\det(\mathbf{M} - s\,\mathbf{I}) = \begin{vmatrix} \rho_- - s & i & 0 \\ -i & -s & i \\ 0 & -i & \rho_+ - s \end{vmatrix}$$

$$= s^3 - 2\rho s^2 + [\rho^2 (1 - \beta^2) - 2]\, s + 2\rho = 0. \tag{C7}$$

The coefficient matrix

$$\mathbf{M} = \begin{pmatrix} \rho_- & i & 0 \\ -i & 0 & i \\ 0 & -i & \rho_+ \end{pmatrix} \tag{C8}$$

of (C6) is Hermitian. Its real eigenvalues s_1 , s_2 , s_3 are the real roots of the cubic equation (C7). In this so-called 'irreducible case' the three real roots cannot be extracted by Cardan's algebraic formula without a circuitous passage into the domain of complex numbers [72]. Hence, those three eigenvalues cannot be represented by simple and elegant expressions.

The system for the components of the eigenvectors (99) explicitly reads :

$$\begin{aligned} (\rho_- - s_k)\, A_{-1}^{(k)} + i\, A_0^{(k)} &= 0, \\ -i\, A_{-1}^{(k)} - s_k\, A_0^{(k)} + i\, A_1^{(k)} &= 0, \\ -i\, A_0^{(k)} + (\rho_+ - s_k)\, A_1^{(k)} &= 0, \quad k = 1,2,3. \end{aligned} \tag{C9}$$

Its solution may be written as

$$A_{-1}^{(k)} = \frac{i}{s_k - \rho_-}\,, \qquad k = 1,2,3, \qquad A_1^{(k)} = -\frac{i}{s_k - \rho_+}\,, \tag{C10}$$

after selecting

$$A_0^{(k)} = 1\,, \qquad k = 1,2,3. \tag{C11}$$

The amplitudes of the diffracted light waves now become

$$\phi_n(\zeta) = \sum_{k=1}^{3} C_k A_n^{(k)} \exp\left(\frac{1}{2} i s_k \zeta\right), n = -1,0,1, \tag{C12}$$

wherein the arbitrary constants will be determined from the boundary conditions (C2). Therefore,

$$\begin{aligned} C_1 A_{-1}^{(1)} + C_2 A_{-1}^{(2)} + C_3 A_{-1}^{(3)} &= 0, \\ C_1 + C_2 + C_3 &= 1, \\ C_1 A_1^{(1)} + C_2 A_1^{(2)} + C_3 A_1^{(3)} &= 0. \end{aligned} \tag{C13}$$

Taking into account (C10) and (C11) we obtain

$$\begin{aligned} C_1 &= \frac{(s_1 - \rho_+)(s_1 - \rho_-)}{(s_1 - s_2)(s_1 - s_3)}, \\ C_2 &= \frac{(s_2 - \rho_+)(s_2 - \rho_-)}{(s_2 - s_1)(s_2 - s_3)}, \\ C_3 &= \frac{(s_3 - \rho_+)(s_3 - \rho_-)}{(s_3 - s_1)(s_3 - s_2)}. \end{aligned} \tag{C14}$$

The calculation of the intensities for $n = -1,0,1$ from (102) is now straightforward. We put $N = 1$, use (C10), (C11) and (C14), and finally set $z = L$ (or $\zeta = v$), to obtain

$$I_{-1} = 4\left[\frac{(s_1 - \rho_+)(s_2 - \rho_+)}{(s_1 - s_2)^2 (s_1 - s_3)(s_2 - s_3)} \sin^2(s_1 - s_2)\frac{v}{4} + \text{cycl.}\right] \tag{C15}$$

$$I_0 = 1 + 4\left[\frac{(s_1 - \rho_+)(s_1 - \rho_-)(s_2 - \rho_+)(s_2 - \rho_-)}{(s_1 - s_2)^2 (s_1 - s_3)(s_2 - s_3)} \sin^2(s_1 - s_2)\frac{v}{4} + \text{cycl.}\right] \tag{C16}$$

$$I_{+1} = 4\left[\frac{(s_1 - \rho_-)(s_2 - \rho_-)}{(s_1 - s_2)^2 (s_1 - s_3)(s_2 - s_3)} \sin^2(s_1 - s_2)\frac{v}{4} + \text{cycl.}\right]. \tag{C17}$$

We just recovered Nagabhushana Rao's results [65], written in a slightly more explicit form. Judged by the occurrence of ρ_+ in the expression for I_{-1} and ρ_- in the formula for I_{+1}, the diffraction spectrum is asymmetric with respect to the zeroth order line. Nagabhushana Rao considered the case $\rho = 1$, which allows for further simplifications. We find it more interesting to look at the case $\beta = \pm 1$, corresponding to light incident at exactly the first Bragg angles. For $\beta = -1$ we have $\varphi = \varphi_{BR}^{(1)}$, $\rho_- = 2\rho$ and $\rho_+ = 0$; the characteristic equation (C7) then simplifies to

$$s^3 - 2\rho s^2 - 2s + 2\rho = 0, \tag{C18}$$

and the intensities become,

$$I_{-1} = 4\left[\frac{s_1 s_2}{(s_1 - s_2)^2 (s_1 - s_3)(s_2 - s_3)} \sin^2 (s_1 - s_2)\frac{v}{4} + \text{cycl.}\right], \tag{C19}$$

$$I_0 = 1 + 4\left[\frac{s_1 s_2 (2\rho - s_1)(2\rho - s_2)}{(s_1 - s_2)^2 (s_1 - s_3)(s_2 - s_3)} \sin^2 (s_1 - s_2)\frac{v}{4} + \text{cycl.}\right], \tag{C20}$$

$$I_{+1} = 4\left[\frac{(2\rho - s_1)(2\rho - s_2)}{(s_1 - s_2)^2 (s_1 - s_3)(s_2 - s_3)} \sin^2 (s_1 - s_2)\frac{v}{4} + \text{cycl.}\right] \tag{C21}$$

If $\beta = 1$, then $\varphi = \varphi_{BR}^{(-1)} = -\varphi_{BR}^{(1)}$, $\rho_- = 0$, $\rho_+ = 2\rho$, so that the characteristic equation remains the same as in (C18). Regarding the intensities, I_{-1} will now be given by the RHS of (C21), and I_{+1} matches the RHS of (C19). Hence,

$$I_{-1}(v\,;\varphi_{BR}^{(-1)}) = I_{+1}(v\,;\varphi_{BR}^{(1)}), \tag{C22}$$

$$I_{+1}(v\,;\varphi_{BR}^{(-1)}) = I_{-1}(v\,;\varphi_{BR}^{(1)}), \tag{C23}$$

a property already established by the general theory [68].

SAMENVATTING

In het eerste deel van deze studie, verschenen in Jaargang 50 nummer 1 van dit tijdschrift, werden benaderde en numerieke methoden in het akoestooptisch diffractievraagstuk behandeld in het geval dat de voortplantingsrichtingen van het invallend licht en van de ultrageluidsgolf loodrecht op elkaar staan. In het tweede deel worden benaderde en numerieke methoden onderzocht in het geval van schuine inval van het licht, d.w.z. dat de voortplantingsrichting van de invallende lichtbundel een hoek φ insluit met de golffronten van de ultrageluidsgolf. Dit geval van schuine inval van het licht verschilt in twee belangrijke aspekten van het geval van loodrechte inval :

(1) Terwijl bij loodrechte inval het diffractiespectrum steeds symmetrisch is t.o.v. de nulde orde ($I_{-n} = I_n$), is dit niet steeds het geval bij schuine inval, waar $I_{-n} \neq I_n$ als regime parameter $\rho = 2\varepsilon_r\lambda^2/\varepsilon_1\lambda^{*2} \neq 0$; slechts voor $\rho = 0$ heeft men een symmetrisch spectrum.
(2) Als we een intensiteit van een bepaalde orde, bv. de p^e orde, beschouwen als een functie van de invalshoek φ, dan zal deze intensiteit een extremum vertonen voor de hoek $\varphi_{BR}^{(p)} = p\lambda/2\lambda^*$, de Bragg hoek van de p^e orde genoemd.

In de inleiding wordt het basisstelsel van differentie-differentiaalvergelijkingen van Raman-Nath herhaald en wordt Brillouin's intuïtieve verklaring weergegeven voor de selectieve Bragg diffractie (of reflectie). In paragraaf 6 worden enkele benaderde methoden in het geval van schuine inval van het licht behandeld.

(1) Als eerste bespreken we de benaderde theorie van Brillouin en Debye, steunend op de methode van de vertraagde potentialen, die een spectrum oplevert met enkel de nulde en eerste orde lijnen. Deze theorie is nochtans van belang aangezien ze de voornaamste fysische kenmerken van het spectrum weergeeft : Doppler verschuiving bij de eerste orde lijnen, richtingen van de gediffracteerde golven en vooral een verklaring voor het optreden van een maximum van de intensiteit van de eerste orde I_{+1} indien het licht invalt onder de Bragg hoek $\varphi_{BR} = \lambda/2\lambda^*$. De voorwaarde voor selectieve (Bragg) reflectie ($I_{-1} \approx 0$) kan uitgedrukt worden met behulp van de Klein-Cook parameter als $Q = 2\pi\lambda L/\lambda^{*2} \gtrapprox 2\pi$.

(2) Voor de ruwe benadering met $\rho = 0$ kan het oneindig Raman-Nath stelsel, juist zoals in het geval van loodrechte inval exact worden opgelost. Dit leidt eveneens tot de resultaten die Raman en Nagendra Nath hebben bekomen met hun elementaire geometrisch optische theorie. Ook hier worden de intensiteiten door eenvoudige uitdrukkingen voorgesteld, nl. $I_n = I_{-n} = J_n^2(v_\varphi)$ met $v_\varphi = v \sin(Q\beta/4) \,/\, (Q\beta/4)$, $\beta = (-2a/\rho) \sin\varphi$ en $a = 2\varepsilon_r\lambda/\varepsilon_1\lambda^*$. In dit speciaal geval is het spectrum symmetrisch t.o.v. de nulde orde lijn. Bovendien zijn de intensiteiten symmetrisch t.o.v. $\beta = 0$. Deze benaderde methode geeft geen verklaring voor Bragg diffractie.

(3) Een verbetering van de elementaire theorie van Raman en Nagendra Nath wordt gegeven door een storingsmethode ontwikkeld door Plancke-Schuyten, Mertens en Leroy. Hierbij wordt de amplitude van de n^e orde uitdrukt als een dubbelreeks in ρ en a. De intensiteiten worden berekend tot op termen in a en ρ^2. De term in a is verantwoordelijk voor de asymmetrie van het spectrum en leidt tot een extremum van $I_n(v, \varphi)$ als de invalshoek φ precies gelijk is aan de Bragg hoek van n^e orde is.

(4) De NOA methode (N^e orde approximatie) bestaat er in het RN stelsel te benaderen door de energie in de orden hoger dan de N^e en deze lager dan de $-N^e$ te verwaarlozen. Het Raman-Nath stelsel bevat dan slechts $2N + 1$ vergelijkingen. In 1939 ontwikkelde Nagabhushana Rao deze methode voor het eenvoudig geval $N = 1$. De analytische formules voor I_0, I_{+1} en I_{-1} bij willekeurige φ en voor $\varphi = \varphi_{BR}^{(\pm 1)}$ worden in Appendix C afgeleid.

In Paragraaf 7 wordt de oplossing van het eindig stelsel van $2N + 1$ vergelijkingen, gedefinieerd door de NOA, herleid tot een eigenwaarden vraagstuk waarvan de $(2N + 1) \times (2N + 1)$ Hermitische matrix $2N + 1$ reële eigenwaarden heeft. De intensiteiten van de diffractielijnen kunnen dan elegant uitgedrukt worden als eindige sommen van kwadraten van sinusfuncties die afhangen van v en van de verschillen van de eigenwaarden twee aan twee ; de coëfficiënten zijn functies van de componenten van de eigenvectoren.

In een volgende paragraaf worden numerische resultaten besproken die met de NOA methode werden bekomen :

(1) I_0 en I_{-1} worden als functies van φ voor $Q = 4.28$ en $Q = 8.36$ vergeleken met de experimenten van Mayer. De overeenkomst is uitstekend.
(2) I_0 en I_{-1} worden voor veranderende β vergeleken met de uitgebreide experimentele resultaten van Klein et al, nl. voor $Q = 0.57$, 2.25, 3.74, 6.28 en 9.3. De theoretische krommen passen zich voortreffelijk aan bij de experimentele punten. Uit iedere grafiek blijkt dat I_{-1} een extremum bezit voor de corresponderende Bragg hoek ($\beta = 1$).
(3) Berekeningen van I_0, $I_{\pm 1}$, $I_{\pm 2}$ in functie van v ($Q = 2.25$, $\beta = 1$ en $\beta = 2$) bevestigen de asymmetrie van het spectrum t.o.v. de nulde orde.
(4) Tevens worden I_0 en $I_{\pm 1}$ in functie van β berekend voor $Q = 0.1$, d.w.z. $Q \ll 1$, voor $v = 1{,}2$ en 3. De bekomen krommen vallen volledig samen met de voorstellingen van de kwadratische Bessel functies uit de elementaire theorie van Raman en Nath. We hebben hier volkomen symmetrie t.o.v. $\beta = 0$.

In Paragraaf 9 worden enkele nauw verwante benaderde methoden bondig besproken :

(1) De MNOA methode van Blomme en Leroy.
(2) Het bijzonder geval van Phariseau's berekeningen, nl. voor $M = 0$, $N = 1$.
(3) Numerieke berekeningen voor de intensiteiten van de dominante diffractielijnen.

We vergelijken ondermeer I_0 en I_1 uit de oplossing van Phariseau en I_0, I_{+1} en I_{-1} berekend met de formules van Nagabhushana Rao in functie van v, bij Bragg inval ($\beta = -1$) voor $Q = 9.3$, met de experimentele data van Klein et al. Jammergenoeg zijn de experimentele gegevens enkel beschikbaar voor $v \leqslant 4$. In het interval [0,4] is de overeenkomst met de 1OA methode uitstekend. De overeenkomst met de resultaten van Phariseau is bevredigend. Voor $v > 5$ zijn er tussen beide theoretische resultaten grote afwijkingen, die er op wijzen dat er hier geen sprake meer kan zijn van "zuivere" Bragg reflectie.

Vervolgens worden I_0, I_{+1} en I_{-1} in functie van v berekend met de 1OA methode bij Bragg inval ($\beta = -1$) (Nagabhushana Rao) voor $Q = 10$, 20, 30, 40 en 50. Hoe groter de waarde van Q hoe kleiner de waarden van I_{-1} in het ganse interval $v \in [0,15]$, zodat hier ook aan de voorwaarde voor "zuivere" Bragg reflectie voldaan is. Berekenen we tenslotte I_0, I_{+1} en I_{-1} als functie van v met de 1OA methode bij Bragg inval ($\beta = -1$) voor $\rho = 1$, 5, 10, 20 dan merken we op, dat vanaf $\rho \approx 20$ de orde -1 volledig verdwijnt in het ganse v-interval, zodat er zich hier "zuivere" Bragg reflectie voordoet.

REFERENCES

[55] Blomme E. and Leroy O., *Diffraction of Light by Ultrasound at Oblique Incidence : An Exact 4th-Order Solution*, in : "Acustica", **59**, 1986, p. 183-192.

[56] BLOMME E. and LEROY O., *Diffraction of Light by Ultrasound at Oblique Incidence : A MN-Order Approximation Method*, in : "Acustica", **63**, 1987, p. 83-89.

[57] BRILLOUIN L., *La Diffraction de la Lumière par des Ultrasons*, Act. Sci. et Ind., No 59, Hermann, Paris, 1933.

[58] DEBYE P., *Zerstreuung von Licht durch Schallwellen*, in : "Phys. Z.", **33**, p. 849-856.

[59] DEFEBVRE A., *Etude Théorique et Expérimentale des Phénomènes de Debye et Sears pour de Fortes Modulations d'Amplitude de la Lumière*, in : "Rev. Opt.", **46**, 1967, p. 557-589 ; **47**, 1968, p. 149-172, p. 205-230.

[60] DEFEBVRE A., MERTENS R.A., OTTOY J.-P. and HEREMAN W., *Experimental Testing of Truncated Raman-Nath Solutions*, in : "Proc. Ultrasonics International 87", 1987, p. 78-83.

[61] KLEIN W.R., COOK B.D. and MAYER W.G., *Light Diffraction by Ultrasonic Gratings*, in : "Acustica", **15**, 1965, p. 67-74.

[62] KLEIN W.R., TIPNIS C.B. and HIEDEMANN E.A., *Experimental Study of Fraunhofer Light Diffraction by Ultrasonic Beams of Moderately High Frequency at Oblique Incidence*, in : "J. Acoust. Soc. Am.", **38**, 1965, p. 229-233.

[63] MAYER W.G., *Light Diffraction by Ultrasonic Waves for Oblique Incidence*, in : "J. Acoust. Soc. Am.", **36**, 1964, p. 779-781.

[64] MERTENS R.A., HEREMAN W. and OTTOY J.-P., *Approximate and Numerical Methods in Acousto-Optics, Part I. Normal Incidence of the Light*, in : "Acad. Anal., Med. Kon. Acad. Wetensch., Lett., Sch. Kunst. Belg., Klasse Wetensch.", **50**, 1988, p. 9-50.

[65] NAGABHUSHANA RAO K., *Diffraction of Light by Supersonic Waves — Part I*, in : "Proc. Indian Acad. Sci.", **9A**, 1939, p. 422-446.

[66] PHARISEAU P., *On the Diffraction of Light by Progressive Supersonic Waves. Oblique Incidence : Intensities in the Neighbourhood of the Bragg Angle*, in : "Proc. Indian Acad. Sci.", **44A**, 1956, p. 165-170.

[67] PLANCKE-SCHUYTEN G., MERTENS R. and LEROY O., *The Diffraction of Light by Progressive Supersonic Waves. Oblique Incidence of the Light. I. Approximate Solution of the Raman-Nath Equations*, in : "Physica", **61**, 1972, p. 299-306.

[68] PLANCKE-SCHUYTEN G. and MERTENS R., *The Diffraction of Light by Progressive Supersonic Waves. Oblique Incidence of the Light. II. Exact Solution of the Raman-Nath Equations*, in : "Physica", **62**, 1972, p. 600-613.

[69] POON T.-C. and KORPEL A., *Feynman Diagram Approach to Acousto-Optic Scattering in the Near-Bragg Region*, in : "J. Opt. Soc. Am.", **71**, 1981, p. 1202-1208.

[70] POON T.-C. and KORPEL A., *Comment on 'Diffraction of Light by Ultrasound at Oblique Incidence : An Exact 4-Order Solution'*, in : "Acustica", **63**, 1987, p. 80.

[71] RYTOV S., *Diffraction de la Lumière par les Ultra-sons*, Act. Sci. et Ind., No 613, Hermann, Paris, 1938.

[72] TURNBULL H.W., *Theory of Equations*, Oliver and Boyd, Edinburgh & London, 1947, 4th Edition.

Contents